Fiber and Integrated Optics, 29:21–43, 2010

ISSN: 0146-8030 print/1096-4681 online
DOI: 10.1080/01468030903450179

Taylor & Francis
Taylor & Francis Group

Impact of the Switching Window Shape on the Performance of a Chain of Reamplification, Reshaping, and Retiming All-Optical Regenerators Based on a Non-Linear Gate

MÁRIO R. G. LEIRIA[1] and ADOLFO CARTAXO[1]

[1]Optical Communication Group, Instituto de Telecomunicações, Department of Electrical and Computer Engineering, Instituto Superior Técnico, Lisboa, Portugal

Abstract *The impact of the switching window shape on the performance of a chain of reamplification, reshaping, and retiming all-optical regenerators based on a non-linear gate is investigated numerically. A method to estimate the chain performance that considers the amplitude fluctuations due to timing jitter and noise redistribution along the chain is proposed. The results show that the rectangular switching window is not appropriate for reamplification, reshaping, and retiming regenerators, and the optimum shape of the switching window depends on the number of regenerators of the chain, optical noise power, and timing jitter levels.*

Keywords 3R all-optical regeneration, bit error ratio, noise redistribution, non-linear gate, switching window, timing jitter

1. Introduction

All-optical reamplification, reshaping, and retiming (3R) regeneration can be achieved using non-linear optical gates, among other options [1, 2]. A non-linear optical gate of a 3R regenerator is a three-port gate, where one port is fed by a decision signal, another port by a clock signal obtained from a clock recovery device (CRD), and the regenerated signal is obtained in the third port. Among the different options to achieve non-linear optical gates, optical interferometers are usually used [3]. The most common optical interferometers used in regeneration are the fiber-based non-linear optical loop mirror (NOLM) and Mach-Zehnder interferometer (MZI) with semiconductor optical amplifiers (SOAs) [3].

Regeneration in a non-linear gate occurs because the non-linear gate performs a non-linear transformation between the input and output power of the regenerator [2, 3]. Due to

Received 27 April 2009; accepted 29 October 2009.
Address correspondence to Mário R. G. Leiria, Instituto de Telecomunicações, Instituto Superior Técnico, Torre Norte, piso 10, Av. Rovisco Pais, 1, 1049-001, Lisboa, Portugal. E-mail: Mario.leiria@lx.it.pt

the non-linear transformation, noise redistribution and signal extinction ratio improvement are achieved [3–7]. However, the non-linear noise redistribution changes the frequently assumed Gaussian distribution of the bit '0' and bit '1' signals and disables the use of the standard Q-factor approaches [3–6]. Therefore, other approaches have to be used to estimate the performance of the regenerator. Related to this subject, the impact of the noise non-linear redistribution on performance of a chain of reamplification and reshaping (2R) all-optical regenerators has already been the main subject of several works [3–7].

In the time domain, the power at the non-linear gate input generates a switching window in the non-linear gate [2]. The switching window is applied to the recovered clock signal, modulating the recovered clock signal by the input signal bit sequence, and, therefore, retiming is achieved [2, 8]. The switching window has to be wide enough to correctly modulate the clock pulses and short enough to reduce possible interference from adjacent bits [8, 9]. At high bit rates (>40 Gbit/s), timing jitter starts to impair the regenerator performance [10, 11], because it originates amplitude fluctuations due to the switching window shape [9, 12]. Besides the amplitude fluctuations caused by the timing jitter, the switching window is also corrupted by the noise at the regenerator input, which is redistributed by the non-linear characteristic of the gate. Therefore, both the amplitude fluctuations due to timing jitter and noise redistribution have to be considered in assessing the performance of 3R regenerators, especially at high bit rates. Since the amplitude fluctuations depend on the switching window shape, the switching window shape may play an important role on the design of a transmission system with 3R regenerators.

At high bit rates (>40 Gbit/s), polarization mode dispersion (PMD) and chromatic dispersion (CD) may introduce significant performance degradation [13, 14]. However, the CD effect can be mitigated by using dispersion compensating fibers in addition to automatic tunable dispersion compensators [13], and PMD degradation can be significantly reduced by using PMD compensators [13, 14]. On the other hand, noise redistribution and timing jitter effects depend essentially on the regenerator parameters. Thus, these effects impose an upper bound on the performance of the transmission system with regenerators. That is why only noise redistribution and timing jitter effects are considered in this article. Although the overall system performance is not assessed by considering only the noise redistribution and timing jitter effects, this study is important to gain insight on the limitations and advantages that 3R all-optical regeneration offers. In order to develop a performance assessment method that can be applied to different regenerator types, a reasonably general regenerator equivalent model is considered. However, because of the remarkably different operation of the non-linear devices used to achieve regeneration, an equivalent model valid for all non-linear devices may not exist.

The aim of this article is to numerically investigate the impact of the switching window shape on the performance of a chain of 3R all-optical regenerators based on non-linear gates. A simple method to assess the performance of the chain of regenerators is proposed for regenerators, where the output power does not depend on the derivative of the regenerator input power, as is observed in regenerators based on the Mamyshev gate [15]. The proposed method takes into account the effect of the amplitude fluctuations due to timing jitter and noise redistribution. The paper is organized as follows. Section 2 presents a theoretical analysis of the bit error ratio (BER) at the output of the 3R regenerator. Section 3 presents the numerical method to estimate the BER along a chain of 3R regenerators. Section 4 presents and analyzes the numerical results, and Section 5 presents the conclusion.

2. Theoretical Analysis of the BER at the 3R Regenerator Output

2.1. Regenerator Equivalent Model

To assess the BER at the regenerator output, it is necessary to obtain the statistical distribution of the signal at the regenerator output. This requires the detailed knowledge of the regenerator operation principle and derivation of the dependence of the regenerator output power on the regenerator input power which, for regenerators using a fiber-based NOLM or MZI with SOAs, can be found in [12–17]. In the case of the MZI-based regenerator, the output power has a complex dependence on the regenerator input power, because the regenerator output power depends on the gain and induced-phase of each SOA, which are related to the input power by differential equations [12–17]. As a result, the determination of the noise statistical distribution at the regenerator output is significantly complex. However, some authors model the SOA-based regenerator behavior by an instantaneous input–output characteristic [18]. A similar complexity occurs for the NOLM-based regenerator, when the walk-off between the clock signal and input signal in the loop cannot be neglected, and the input signal shape changes along the propagation in the loop. However, when the walk-off between the clock signal and input signal in the loop can be neglected and the input signal shape does not change along the propagation in the loop, the switching window is related to the optical power at the NOLM input by an instantaneous input–output characteristic. This allows the statistical distribution of the switching window to be obtained from the instantaneous non-linear transformation of the regenerator input power using well-known methods from the probability theory [19]. By these reasons, in the equivalent model, the non-linear transformation is modeled by an instantaneous non-linear input–output characteristic. Otherwise, it would be very complex and difficult to compute the statistical distribution of the switching window, and that distribution would be almost necessarily assessed by Monte Carlo simulation. Furthermore, this equivalent model allows the study of regenerator performance independently from the technology used to achieve regeneration.

Due to the instantaneous non-linear input–output characteristic, the switching window width is similar to the one of the pulse at the non-linear gate input. Therefore, in the equivalent model proposed, a pulse reshaper is assumed at the non-linear gate input in order to set the width of the switching window as considered in [10, 11]. In addition, the pulse reshaper allows for the possibility of controlling the shape of the switching window [10, 11]. Thus, the equivalent model is not absolutely valid for SOA- and NOLM-based regenerators, where the walk-off and change of the input signal shape along the propagation in the loop cannot be neglected. However, it is expected that the equivalent model can still provide qualitative information about the performance of a chain of 3R regenerators based on non-linear gates, when the power at the regenerator output depends only on the power at the regenerator input and not on the derivative of the instantaneous input power.

The block diagram and low-pass equivalent model of the 3R regenerator based on a non-linear gate are, respectively, shown in Figures 1a and 1b. The non-linear gate is modeled as a power detector, followed by a non-linearity (which performs the noise and signal non-linear redistribution and is described by $F_{NL}(x)$) and a block responsible for the multiplication of the clock signal and the non-linear redistribution signal as described in [2]. The pulse reshaper is modeled by a linear filter [20]. The optical filter

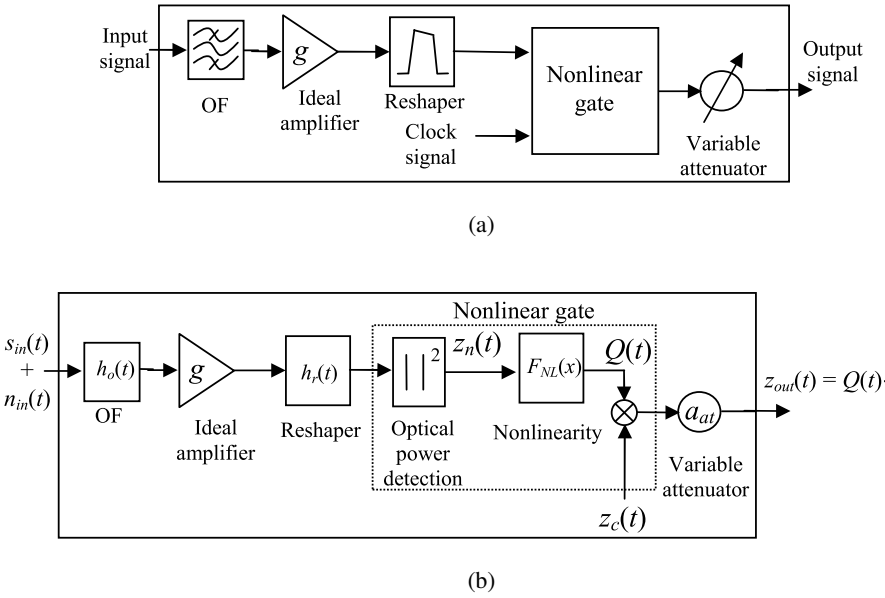

Figure 1. (a) 3R regenerator based on a nonlinear gate. (b) Regenerator low-pass equivalent model where $z_{out}(t)$, $z_n(t)$, and $z_c(t)$, are, respectively, the power at the regenerator output, at the non-linearity input, and of the recovered clock signal normalized by the maximum signal power of bit '1' at the transmitter output. $s_{in}(t)$ and $n_{in}(t)$ are, respectively, the low-pass equivalent of the optical field of the input signal and noise normalized by the square root of the maximum signal power of bit '1' at the transmitter output, and $Q(t)$ is the transmittance of the non-linear gate. OF stands for optical filter, and a linear and fixed polarization state is assumed in front of the regenerator.

at the regenerator input is responsible for noise reduction, the ideal amplifier adjusts the non-linearity threshold, and the variable attenuator is used to maintain the same average power at each regeneration section input [4]. A linear and fixed polarization state is assumed in front of the regenerator in this article. Furthermore, any chirping effect from the non-linear gate is neglected, and it is assumed that the regenerator output signal field has a constant phase.

2.2. *Impact of Noise and Timing Jitter on the BER*

To illustrate the regenerator operation, Figure 2 shows a scheme of the evolution of the pulses along the main stages of the regenerator. In the presence of timing jitter, both the regenerator input signal and recovered clock signal are corrupted by timing jitter. In the absence of noise, the optical field of the signal at the regenerator input is assumed to be composed by linearly superimposed pulses. Designating by $\tau_{s,k}$ the timing jitter of the kth input pulse, the optical field of the regenerator input signal can be written as $s_{in}(t) = \sum_{k=-\infty}^{+\infty} b_k \cdot s_p(t - kT - \tau_{s,k})$, where b_k is the amplitude of the kth bit normalized by $\sqrt{P_1}$, P_1 is the peak power of bit '1' at the transmitter output, T is the bit time period, $s_p(t)$ is the shape of the signal pulse with $\max\{|s_p(t)|^2\} = 1$, and $\max\{x\}$ is the maximum value of x. At the non-linearity input, the normalized signal power is

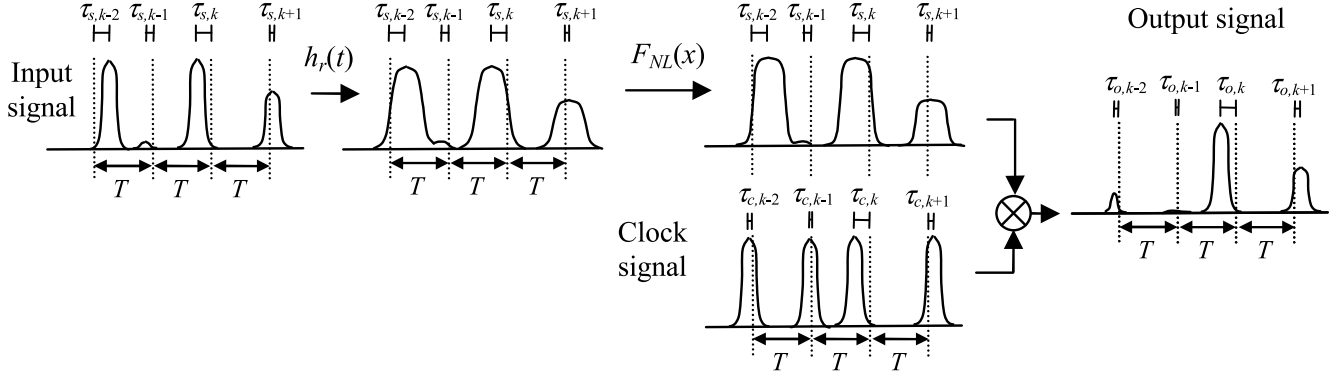

Figure 2. Example of pulses along the different stages of the 3R all-regenerator in the absence of noise. It should be noted that, to illustrate the effect of the jitter, the timing jitter is shown changing from pulse to pulse. The different amplitudes of the input pulses result from a non-ideal decision made by the previous regenerators in the chain.

given by

$$z_n(t) = g\left|\sum_{k=-\infty}^{+\infty} b_k \cdot s_p(t-kT-\tau_{s,k}) * h_o(t) * h_r(t) + n_{in,p}(t) * h_o(t) * h_r(t)\right|^2$$

$$= g\left|\sum_{k=-\infty}^{+\infty} b_k \cdot s_r(t-kT-\tau_{s,k}) + n(t)\right|^2, \quad (1)$$

where $n_{in,p}(t)$ is the low-pass equivalent of the optical field of the noise at the regenerator input in the polarization direction of the polarizer and normalized by $\sqrt{P_1}$, $s_r(t) = s_p(t) * h_o(t) * h_r(t)$, $n(t) = n_{in,p}(t) * h_o(t) * h_r(t)$, g is the power gain of the ideal amplifier, $h_o(t)$ is the low-pass equivalent impulse response of the optical filter at the regenerator input, $h_r(t)$ is the low-pass equivalent impulse response of the pulse reshaper, and $*$ stands for convolution.

The recovered clock signal is assumed to be composed by linearly superimposed pulses in amplitude with a time duration much shorter than T. Its power is approximately given by $z_c(t) = \sum_{w=-\infty}^{+\infty} |d|^2 \cdot |s_{c,p}(t-wT-\tau_{c,w})|^2$, where d is the amplitude of the clock pulses normalized by $\sqrt{P_1}$, $\tau_{c,w}$ is the timing jitter of the wth pulse, and $s_{c,p}(t)$ is the shape of the clock pulses with $\max\{|s_{c,p}(t)|^2\} = 1$.

Due to the low-pass jitter transfer function of the CRDs, usually with a cut-off frequency around hundreds of kHz [21], $\tau_{s,k}$ and $\tau_{c,w}$ are slowly varying stochastic processes. As a consequence, the timing jitter of the ith signal pulse $\tau_{s,i}$ and the ith clock pulse $\tau_{c,i}$ hold $\tau_{s,i} \approx \tau_{s,w+i}$ and $\tau_{c,i} \approx \tau_{c,w+i}$ for w of the order of thousands when the bit rate is of the order of or exceeds 1 Gb/s. Thus, for mathematical convenience, in the time interval over which $\tau_{s,i} \approx \tau_{s,w+i}$ and centered at the ith signal pulse, the noise can be expanded as $n(t) \approx \sum_w n_w(t-wT-\tau_{s,i})$. Therefore, neglecting the small superposition between two adjacent pulses after the pulse reshaper, the transmittance of the non-linear gate can be approximated by

$$Q(t) = F_{NL}(z_n(t)) \approx \sum_{w=-\infty}^{+\infty} q_w(t-wT-\tau_{s,i}), \quad (2)$$

where $q_w(t)$ is the switching window associated with the wth bit, given by

$$q_w(t) = F_{NL}(g|b_w|^2|s_r(t)|^2 + g|n_w(t)|^2 + 2g\,\mathrm{Re}(b_w s_r(t) n_w^*(t))), \quad (3)$$

where $\mathrm{Re}(x)$ stands for the real part of x, and x^* is the complex conjugate of x. Assuming that each switching window only affects one clock pulse, the regenerator output signal power can be written as

$$z_{out}(t) = \frac{\sum_w |d|^2 |s_{c,p}(t-wT-\tau_{c,i})|^2 q_w(t-wT-\tau_{s,i})}{a_{at}}, \quad (4)$$

where a_{at} is the loss of the variable attenuator.

Factoring out the intensity of the switching windows at the time instant of the maxima of the clock signal pulses $t = wT + \tau_{c,i}$, the switching window can be written as

$$q_w(t - wT - \tau_{s,i}) = \frac{q_w(\tau_{c,i} - \tau_{s,i}) \cdot q_w(t - wT - \tau_{s,i})}{q_w(\tau_{c,i} - \tau_{s,i})}$$
$$= q_w(\tau_{c,i} - \tau_{s,i}) \cdot q_w^{\iota}(t - wT - \tau_{s,i}), \tag{5}$$

where $q_w^{\iota}(t)$ is the normalized switching window associated with the wth clock pulse with an amplitude of 1 at the time instant of the wth clock pulse maximum. Thus, replacing expression (5) in expression (4), the regenerator output power is given by

$$z_{out}(t) = \frac{\sum_w |d|^2 \cdot q_w(\tau_{c,i} - \tau_{s,i}) \cdot |s_{c,p}(t - wT - \tau_{c,i})|^2 \cdot q_w^{\iota}(t - wT - \tau_{s,i})}{a_{at}}, \tag{6}$$

which can be written as

$$z_{out}(t) = \sum_w a_{out,w} \cdot g_{out,w}(t - wT - \tau_{o,w}), \tag{7}$$

where $\tau_{o,w}$ is the timing jitter of the regenerator output signal associated with the wth bit, $g_{out,w}(t)$ is the normalized shape of the pulse at the regenerator output associated with the wth transmitted bit given by $g_{out,w}(t - \tau_{o,w}) = |s_{c,p}(t - \tau_{c,i})|^2 \cdot q_w^{\iota}(t - \tau_{s,i})$, and $a_{out,w}$ is given by

$$a_{out,w} = \frac{|d|^2 \cdot q_w(\tau_{c,i} - \tau_{s,i})}{a_{at}}. \tag{8}$$

$g_{out,w}(t)$ describes the shape change of the output signal due to the time misalignment between the clock pulse and the switching window and due to changes of the switching window shape caused by noise. $a_{out,w}$ describes the dependence of the peak power of the output pulse on the timing jitter of the clock signal, on the input signal timing jitter, and on the switching window shape. As the switching window is usually larger than the clock pulse and input signal pulse widths [8], the bandwidth of the amplitude response of the pulse reshaper is narrower than the bandwidth of the input signal or clock signal. As a result, the coherence time of the noise at the non-linearity input is usually higher than the input or clock pulse time widths. Therefore, due to the strong correlation of the noise, in the switching window along the clock pulse duration, the impact of the noise on the signal at the regenerator output is mainly described by $a_{out,w}$. Additionally, it is assumed that the shape of the pulses at the regenerator output is approximately the same as the one obtained in the absence of timing jitter and noise. This means that the pulse shape at the regenerator output is assumed to be weakly affected by noise and timing jitter. Furthermore, the timing jitter of the output signal is approximately the same as the timing jitter of the clock signal, $\tau_{o,w} \approx \tau_{c,i}$ [22].

To estimate the BER at the regenerator output, the probability density function (PDF) of the regenerator output signal at the sampling time instant must be calculated. Assuming that the sampling time instants are the time instants of the recovered clock pulses maxima, from expression (7), it can be concluded that the regenerator output signal at the clock pulse maxima time instants is given by $a_{out,w}$. Expression (8) shows that $a_{out,w}$ depends on $\tau_{c,i} - \tau_{s,i}$, which is known as alignment jitter and is a random variable [23]. Besides

the alignment jitter, the switching window $q_w(t)$ is also corrupted by noise. Since $q_w(t)$ results from the non-linear transformation of the non-linearity input power (as shown by expression (3)), the noise and signal non-linear transformations performed by $F_{NL}(x)$ must also be computed. Assuming that $s_{in}(t)$ is a deterministic signal and that the real and imaginary parts of $n_{in,p}(t)$ are independent Gaussian random variables, the distribution of $z_n(t)$ is a non-central chi-square distribution with two degrees of freedom [24]. The mean and variance of $z_n(t)$ are, respectively, given by $\mu_{z_n}(t) = 2g\sigma_n^2 + z_{n,s}(t)$ and $\sigma_{z_n}^2(t) = 4g^2\sigma_n^4 + 4g\sigma_n^2 z_{n,s}(t)$, where σ_n^2 is the variance of the imaginary and real parts of $n(t)$, $z_{n,s}(t) = \sum_{w=-\infty}^{+\infty} z_{n,s,w}(t - wT) = \sum_{w=-\infty}^{+\infty} g|b_w|^2|s_r(t - wT)|^2$, and $z_{n,s,w}(t)$ is the signal power at the non-linearity input in the absence of noise associated with the wth transmitted bit, given by

$$z_{n,s,w}(t) = g|b_w|^2|s_r(t)|^2. \tag{9}$$

Since $n(t)$ is stationary, the PDF of $Q(t)$ conditioned on $z_{n,s}(t)$ is the same as the PDF of $q_w(t)$ conditioned on $z_{n,s,w}(t)$. Using Eqs. (9) and (3), the PDF of $q_w(t)$ conditioned on $z_{n,s,w}(t)$ is given by [19]

$$f_{q_w}(z|z_{n,s,w}(t)) = f_{z_n}(F_{NL}^{-1}(z)|z_{n,s,w}(t)) \cdot \left| \frac{dF_{NL}^{-1}(y)}{dy} \right|_{y=z}, \tag{10}$$

where $f_{z_n}(z|z_{n,s,w}(t))$ is the PDF of $z_n(t)$ conditioned on $z_{n,s,w}(t)$, and $F_{NL}^{-1}(z)$ is the inverse function of $F_{NL}(x)$. In the absence of timing jitter, $z_{n,s,w}(t)$ is still random because it depends on the randomness of $|b_w|^2$; i.e., it depends on the transmitted bit. As a result, the PDF of $q_w(t)$ conditioned on $z_{n,s,w}(t)$ is also conditioned on the transmitted bit or $|b_w|^2$. It should be noted that, at the first regenerator input, $|b_w|^2$ is equal to 1 when bit '1' is transmitted and equal to the inverse of the extinction ratio of the transmitter when bit '0' is transmitted. In the case of a chain of regenerators, $|b_w|^2$ depends on the transmitted bit and on the decisions made by the previous regenerators.

Assuming the alignment jitter as a stationary process, from expression (8), the PDF of $a_{out,w}$ conditioned on the transmitted bit is obtained by statistically averaging the effect of the alignment jitter of the PDF of $a_{out,w}$ in the absence of timing jitter. Thus, after some mathematical manipulation and using expression (8), the PDF of $a_{out,w}$ conditioned on the transmitted bit 'b' is given by

$$f_{a_{out,w}}(z|\text{`}b\text{'}) = \frac{a_{at}}{|d|^2} \int_{-\infty}^{+\infty} f_{q_w}\left(\frac{a_{at} \cdot z}{|d|^2} \middle| z_{n,s,w}(t) = z_{n,s,w}(u) \right) \cdot f_{jit}(u)du, \tag{11}$$

where $f_{jit}(u)$ is the PDF of the alignment jitter. Then, replacing expression (10) into expression (11), the PDF of $a_{out,w}$ conditioned on the transmitted bit 'b' is given by

$$f_{a_{out,w}}(z|\text{`}b\text{'}) = \frac{a_{at}}{|d|^2} \int_{-\infty}^{+\infty} \left| \frac{dF_{NL}^{-1}(y)}{dy} \right|_{y=\frac{a_{at}\cdot z}{|d|^2}} f_{jit}(u) \cdot f_{z_n}\left(F_{NL}^{-1}\left(\frac{a_{at} \cdot z}{|d|^2} \right) \middle| z_{n,s,w}(t) = z_{n,s,w}(u) \right) du. \tag{12}$$

Further simplification of expression (12) is achieved by making the substitution $v = z_{n,s,w}(u)$. However, $z_{n,s,w}(t)$ is non-monotonic. As a consequence, $z_{n,s,w}(t)$ is divided into

C_p monotonic parts, with the cth part designated as $z_{n,s,w,c}(t)$ and $1 \le c \le C_p$. Thus, making the substitution $v_c = z_{n,s,w,c}(u)$ in the cth monotonic part, for $1 \le c \le C_p$, the PDF of $a_{out,w}$ conditioned on the transmitted bit 'b' is given by

$$f_{a_{out,w}}(z|\text{`}b\text{'}) = \frac{a_{at}}{|d|^2} \sum_{c=1}^{C_p} \left| \int_{z^{-1}_{n,s,w,c}(t_{c,-})}^{z^{-1}_{n,s,w,c}(t_{c,+})} f_{z_n}\left(F^{-1}_{NL}\left(\frac{a_{at} \cdot z}{|d|^2} \right) \middle| z_{n,s,w}(t) = v_c \right) \right.$$

$$\left. \cdot \left| \frac{dF^{-1}_{NL}(y)}{dy} \right|_{y=\frac{a_{at} \cdot z}{|d|^2}} \cdot \left| \frac{dz^{-1}_{n,s,w,c}(y)}{dy} \right|_{y=v_c} f_{jit}(z^{-1}_{n,s,w,c}(v_c)) dv_c \right|, \quad (13)$$

where $t_{c,+}$ and $t_{c,-}$ are, respectively, the upper and lower limits of the cth monotonic function. The modulus was inserted in each term of the sum of expression (13), because each probability contribution cannot be negative. Otherwise, the integration limits would have to be changed depending if $z_{n,s,w,c}(t)$ is an increasing or decreasing function.

From expression (13), assuming equally likely distributed transmitted bits at the regenerator chain input, the BER at the regenerator output is given by

$$BER = \frac{1}{2} \cdot \int_0^{v_{th}} f_{a_{out,w}}(v|\text{`}1\text{'}) dv + \frac{1}{2} \cdot \int_{v_{th}}^{+\infty} f_{a_{out,w}}(v|\text{`}0\text{'}) dv, \quad (14)$$

where v_{th} is the optimum decision threshold calculated from the equation

$$f_{a_{out,w}}(v_{th}|\text{`}1\text{'}) = f_{a_{out,w}}(v_{th}|\text{`}0\text{'}).$$

3. Computation of the BER in a Chain of 3R Regenerators

The optical transmission system with 3R regenerators is composed by a chain of regeneration sections, as shown in Figure 3, where m is the number of regeneration sections. Each regeneration section is composed by a cascade of optical fiber spans and optical amplifiers and a 3R all-optical regenerator [3–5]. As in [3–7], it is assumed that the optical amplifiers compensate for any losses in the regeneration section and a dispersion compensation scheme is used in each regeneration section to compensate for the CD effect. Since high-speed transmission is usually performed in the quasi-linear transmission regime and dispersion reduces the peak power of the pulses along the regeneration section [13], the peak power of the pulses is not high along the regeneration section. For these reasons, in this article, the distortion effects due to fiber non-linearity and dispersion are neglected, and attention is dedicated to noise redistribution and timing jitter effects associated with the 3R regenerator operation. Therefore, the cascade of fiber spans, optical amplifiers, and dispersion compensators is modeled by a block, where only optical noise is added to the signal.

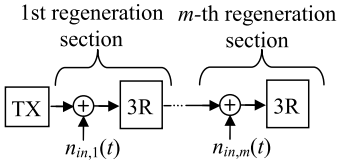

Figure 3. Equivalent scheme of a transmission system with 3R regenerators, where $n_{in,k}(t)$ is the optical noise added in the kth regeneration section ($1 \le k \le m$).

3.1. Signal Description along the Chain of Regenerators

As previously discussed, it is assumed that all 3R regenerator output pulses have the same shape but different amplitudes, given by $a_{out,w}$ and timing jitter, $\tau_{o,w}$, as shown in expression (7). As a consequence, along the chain, the signal at the regenerator input is composed by pulses with the same shape but different amplitudes $|b_w|^2$ and timing jitter $\tau_{s,w}$. Since distortion effects due to fiber non-linearity and dispersion are neglected and the losses in the regeneration section are compensated, the peak power of the wth signal pulse at the kth regenerator input is given by $|b_{w,k}|^2 = a_{out,w,k-1}$, where $a_{out,w,k-1}$ is the $(k-1)$th regenerator output peak power of the wth pulse, and the timing jitter is given by $\tau_{s,w,k} = \tau_{o,w,k-1}$, where $\tau_{o,w,k-1}$ is the timing jitter of the wth pulse at the $(k-1)$th regenerator output.

To estimate the BER along the regeneration chain, the PDFs of the regenerator output signal at the clock pulses maxima time instants $a_{out,w}$, when bits '0' and '1' are transmitted, must be computed along the regenerator chain. However, the kth regenerator PDF of $a_{out,w}$ depends on the PDF of $a_{out,w}$ of the previous regenerator. As the PDF of $a_{out,w}$ does not have a closed-form expression, numerical or approximated methods are required to estimate the PDF of $a_{out,w}$ along the regenerator chain.

3.2. BER Estimation along the Chain of Regenerators

The method used to estimate the PDFs of the regenerator output signal at the clock pulses maxima time instants $a_{out,w}$ along the regenerator chain is a generalization of the method proposed in [7]. In this method, the PDFs of $a_{out,w}$ are discretized, and the 2R regeneration process of the regenerator is described by a probability transfer matrix. However, the method proposed in [7] was only developed for a chain of 2R regenerators. It has to be modified in order to be used in a chain of 3R regenerators, where the alignment jitter affects the way of computing the PDFs.

In order to estimate the PDFs of $a_{out,w}$ along the chain, the 3R regenerator output power and signal power at the non-linearity input, in the absence of noise, are approximated by upper and under stair-case functions. The stair-case approximations allow describing the 3R regeneration process of the regenerator by a probability transfer matrix and the PDF of $a_{out,w}$ by a probability vector. As the probability vector of $|b_w|^2$ at the first regenerator is known, it is possible to estimate the probability of $a_{out,w}$ by multiplying the probability transfer matrix of the regenerators along the chain by the probability vector of $|b_w|^2$ at the first regenerator input. Finally, after converting the probability vector of $a_{out,w}$ into a discrete PDF, the BER is computed using expression (14). The derivation and details of the proposed method can be found in Appendix A.

4. Results and Analysis

The impact of the switching window shape on the performance of the regenerator chain is investigated for a chain of 3R all-optical regenerators based on a NOLM with a pulse reshaper. As previously stated, the proposed method can be applied to other types of regenerators different from the NOLM-based regenerator as long as they can be described by an instantaneous input–output characteristic. In this article, only the case of the NOLM-based 3R all-optical regenerators with pulse reshaper is studied.

In order to apply the proposed method to NOLM-based 3R all-optical regenerators, the non-linear characteristic of the NOLM has to be determined. The NOLM scheme is

shown in Figure 4a. In the case of a negligible walk-off between the input signal and co-propagating clock signal in the NOLM, the non-linear characteristic of the NOLM was presented in [12] and it is given by

$$F_{NL}(x) = 1 - 4K \cdot (1 - K) \cos^2(\gamma L \cdot P_1 \cdot x/2), \tag{15}$$

where K is the power coupling ratio of the 2×2 coupler ($0 \leq K \leq 1$), γ is the fiber non-linear coefficient, x is the normalized power at the NOLM input, and L is the loop fiber length. In expression (15), the effect of cross-phase modulation induced by the input signal on the clock pulses that counter-propagate with respect to the input signal is neglected. This effect causes a reduction of the extinction ratio of the non-linear characteristic when the duty-cycle and bit rate of the input signal are high [25]. However, it can be mitigated by properly designing the NOLM [25].

The non-linear characteristic of the NOLM is shown in Figure 4b. The power coupling ratio is related to the regenerator extinction ratio in dB, r_{NL}, by $K = 1/2 + 1/2 \cdot 10^{-r_{NL}/20}$. The length of the optical fiber in the loop is set so that $\gamma L \cdot P_1 = \pi$. Therefore, the first maximum of the non-linear characteristic of the NOLM occurs for $x = 1$, and the non-linear threshold (x_{th}), defined as the point of the maximum slope of the non-linear characteristic for $x < 1$ [4], occurs at $x_{th} = 1/2$. However, due to the ideal amplifier, the effective non-linearity threshold affecting the power at the regenerator input is $x_{th,NL} = 1/(2g)$, and the maximum of the non-linear characteristic

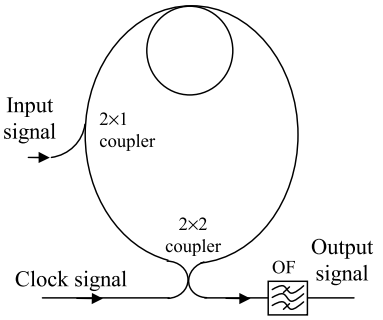

(a)

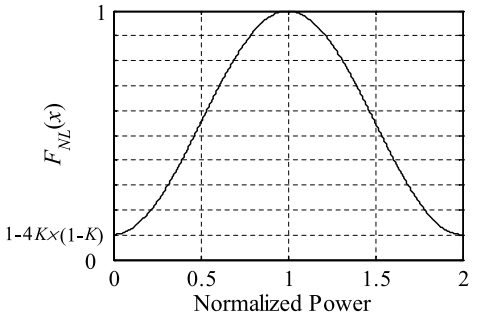

(b)

Figure 4. (a) Scheme of a NOLM, where OF stands for optical filter; (b) non-linear characteristic of the NOLM.

affecting the regenerator input power occurs at $1/g$. The non-linearity extinction ratio r_{NL} and the transmitter extinction ratio are assumed to be 20 dB, which is a realistic value for an optical transmission system with regenerators [3].

The pulse reshaper at the regenerator input allows the obtaining of different shapes of the pulse at the NOLM input and, therefore, different switching windows. In this study, three different pulse shapes at the NOLM input are considered: rectangular, Gaussian, and second-order super-Gaussian. The second-order super-Gaussian shape was chosen because it is similar to the flat-top shape experimentally obtained in [10, 11, 20]. The Gaussian shape was chosen to understand the impact of a non-flat-top switching window on the regenerator performance. In the case of the rectangular switching window, it is often implicitly considered by other authors as the optimum switching window shape to increase the timing jitter tolerance of a 3R regenerator [10, 11, 20, 22]. Therefore, its impact on the BER should be compared with the impact of other more realistic shapes of the switching window. The transfer function of the pulse reshaper is obtained from the relation between the spectrum of the optical field of the target pulse at the NOLM input and the spectrum of the optical field of the reference pulse at the reshaper input.

Due to the filtering effect of the pulse reshaper, both noise and signal at the NOLM input are modified by the pulse reshaper transfer function. As the transfer function of the pulse reshaper depends on both the target pulse at the NOLM input and the reference pulse at the reshaper input, the variance of the noise at the pulse reshaper output depends on the shape and full-width at half maximum (FWHM) of the target pulse at the NOLM input D_{sw}. Therefore, to understand the impact of the amplitude fluctuations due to alignment jitter on the performance of the regenerator chain, the noise variance at the NOLM input is set to be the same, independent of the pulse reshaper transfer function. This condition is ensured by increasing or decreasing the noise added in the regeneration section. This allows comparing the performance of the different switching window shapes for the same BER degradation due to the noise. The realistic situation, where the noise added in the regeneration section is assumed constant, will be presented in a future work. The noise variances are set so that the BER at the NOLM input is 10^{-30} (case 1), 10^{-20} (case 2), and 10^{-12} (case 3).

The alignment jitter is assumed to have a Gaussian distribution with a variance given by σ_j^2 [9]. The power of the signal at the CRD output is assumed to be composed by Gaussian-shaped pulses with FWHM D_c of $0.2 \cdot T$ and a bit rate of 160 Gbit/s. The optical filter at the regenerator input has a fourth-order super-Gaussian amplitude response, and the -3-dB bandwidth of the filter was set to be six times the bit rate. This -3-dB bandwidth was chosen in order to obtain a second-order super-Gaussian shaped pulse at the NOLM input with $D_{sw} = 0.5 \cdot T$ $(2.5 \cdot D_c)$ with reduced amplitude distortion. Identical $x_{th,NL}$ and pulse reshaper transfer functions are assumed along the chain. To ensure that the switching window of all regenerators along the chain is the same in the absence of noise and timing jitter, it is assumed that the signal at the transmitter output results from the product of the target switching window, when bit '1' is transmitted and in the absence of noise, and a clock signal.

4.1. Method Validation

To validate the proposed method to estimate the BER along the chain of regenerators, the PDFs of $a_{out,w}$ for each bit estimated by the proposed method are compared with PDFs of $a_{out,w}$ estimated using Monte Carlo simulation. The proposed method assumes that

the signal shape at the regenerator output does not change, in the presence of noise and alignment jitter, from regenerator to regenerator along the chain for similar regenerator. However, in the presence of noise and alignment jitter, the pulses at the regenerator output suffer from asymmetries due to the product of the switching window by the clock signal. In order to gain insight on the limitations of this approximation, different FWHMs of the clock pulse are considered in the Monte Carlo simulations.

Results have shown that, in addition to the jitter of the output signal resulting from the clock timing jitter, the product of the switching window by the clock pulse adds timing jitter to the regenerator output signal when a time misalignment between the switching window and clock pulses occurs. This timing jitter corresponds to the transference of alignment jitter to timing jitter by the switching window. However, since the alignment jitter is a low-pass stochastic process, the timing jitter resulting from the alignment jitter transference will have variations that can be tracked by the CRD. Thus, this type of timing jitter does not lead to alignment jitter in the following regenerator and will not introduce BER degradation. In this analysis, the impact of this effect on the BER was suppressed. In order to realize a rigorous comparison between the Monte Carlo and proposed method estimates, a_{at} computed in the proposed method is used in the Monte Carlo simulation.

Figure 5 shows the PDF of $a_{out,w}$ estimated by the proposed method and by Monte Carlo simulation with different FWHMs of the clock pulse for different switching window shapes. The results have shown that the PDF estimated by the proposed method does not match the PDF of $a_{out,w}$ along the regenerators chain ($m > 1$). The estimate discrepancies result from the BER variation caused by the change of the shape of the regenerator output pulse due to the product between clock pulses and switching windows corrupted by noise and alignment jitter. However, for a small number of regenerators ($m < 7$) or when the FWHM of the clock pulse is low ($\leq 0.1 \cdot T = 0.2 \cdot D_{sw}$), the results showed that the discrepancy of the BER estimates of the proposed method is lower than one order of magnitude. This is confirmed in Figure 6, where the BER estimated by the proposed method and by Monte Carlo simulations is shown for $m \geq 7$. BER estimates for $m < 7$

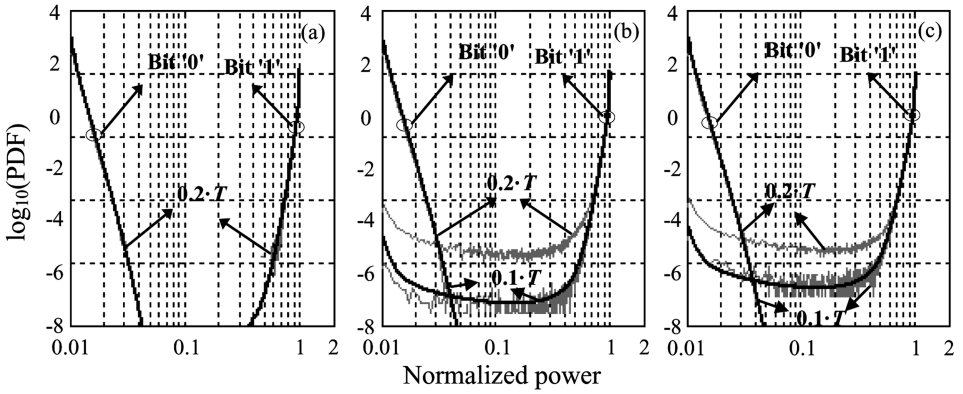

Figure 5. PDF of $a_{out,w}$ for a second-order super-Gaussian shaped [(a) and (b)] and Gaussian-shaped (c) pulse at the NOLM input, $D_{sw} = 0.5 \cdot T$ (case 1) and $\sigma_j = 0.3$ ps. Gray lines correspond to Monte Carlo simulations for different FWHMs of the clock pulses and the black line to the proposed method: (a) $m = 1$, (b) and (c) $m = 10$; (a) and (b) $x_{th,NL} = 0.48$, (c) $x_{th,NL} = 0.47$.

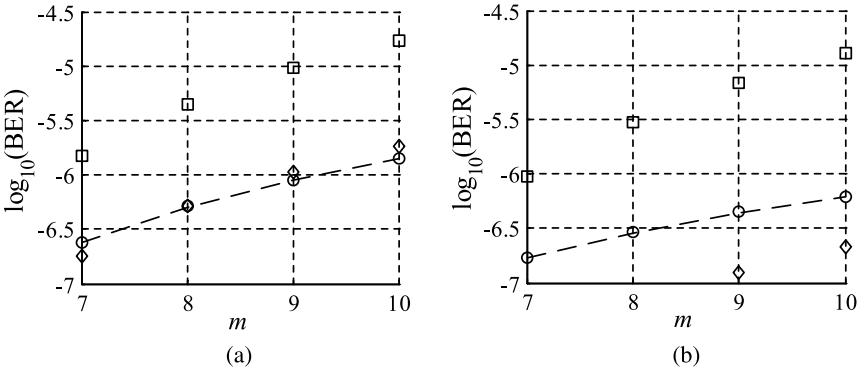

Figure 6. $\log_{10}(BER)$ as a function of m for $D_{sw} = 0.5 \cdot T$ (case 1) and $\sigma_j = 0.3$ ps: (a) Gaussian-shaped pulse at the NOLM input, $x_{th,NL} = 0.47$; (b) super-Gaussian shaped pulse at the NOLM input, $x_{th,NL} = 0.48$. Dashed line, BER estimated by the proposed method; marks, BER estimated by Monte Carlo simulation; circles correspond to Dirac-shaped clock pulses; diamonds correspond to clock pulses with an FHWM of $0.1 \cdot T$ $(0.2 \cdot D_{sw})$; and squares correspond to clock pulses with an FHWM of $0.2 \cdot T$ $(0.4 \cdot D_{sw})$. Note that BERs lower than 10^{-7} are not shown because of the low accuracy of the Monte Carlo simulation, which results from not having enough realizations in the Monte Carlo simulations.

are not shown due to the reduced accuracy of the Monte Carlo simulation. Figure 6 shows that the BER discrepancy is only higher than one order of magnitude for $m \geq 8$. It should be stressed that, at the output of the first regenerator and for Dirac-shaped delta clock pulses, the estimates of the proposed method exactly match the Monte Carlo simulation results.

The effect of the change of the shape of the regenerator output pulse is not considered in the following results. An improvement of the present method is required to take into account the BER variation caused by the changes of the shape of the regenerator output pulses.

4.2. Impact of Timing Jitter and Noise on the BER of 3R Regenerators

Figure 7a shows the BER at the output of the mth regenerator for different shapes of the pulse at the NOLM input $\sigma_j = 600$ fs, $D_{sw} = 0.75 \cdot T$ $(3.75 \cdot D_c)$, and case 1. Comparing the BER in the absence and presence of alignment jitter, it can be seen that the degradation caused by the alignment jitter is much higher than the degradation caused by the noise. In this situation, the high variance of the alignment jitter makes the alignment jitter the dominant source of BER degradation. For higher noise power, Figures 7b and 7c show that as the noise power increases, the alignment jitter may not be the main dominant source of BER degradation and, after a certain number of regenerators, the noise accumulation dominates the BER degradation. It should be noted that the small BER degradation observed in Figure 7 in the absence of alignment jitter and at the first regenerator output results from the probability fold-back effect that occurs in regenerators with a cosine nonlinear characteristic. This effect has already been studied elsewhere [3, 4]. Comparing the performance of the different shapes considered for the switching window, Figure 7 shows that for small m, the switching window resulting from a Gaussian-shaped pulse at the NOLM input has the lowest BER, and the rectangular switching window has

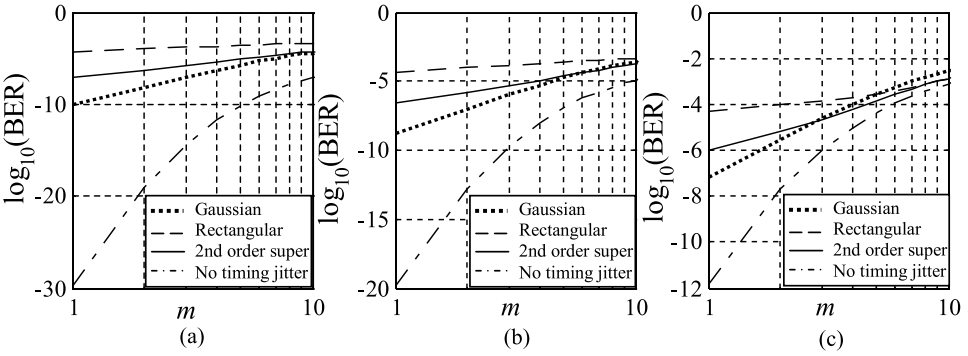

Figure 7. $\log_{10}(BER)$ as a function of m for the optimum $x_{th,NL}$, different shapes of the pulse at the NOLM input, $D_{sw} = 0.75 \cdot T$ $(3.75 \cdot D_c)$ and $\sigma_j = 600$ fs and 0 fs: (a) case 1, (b) case 2, and (c) case 3.

the highest BER, among the analyzed switching window shapes. On the other hand, the increased rate of the BER with m is higher for the switching window resulting from a Gaussian-shaped pulse and lower for the rectangular switching window. To explain these results, Figure 8a shows the PDFs of $a_{out,w}$ at the first regenerator output for different shapes of the pulse at the non-linearity input. It can be observed that the alignment jitter only affects the PDF of bit '1', because the non-linear gate is closed for bit '0'. For a rectangular switching window, Figure 8a shows the appearance of a probability peak for low normalized powers. For higher powers, the PDF follows the PDF in the absence of timing jitter (in order to clarify Figure 8, the PDF in the absence of timing jitter was not shown). This peak occurs when the alignment jitter moves the clock signal pulse (or sampling time instant) to the outside of the switching window. The peak magnitude depends on the probability of the clock pulse falling outside the switching window due to the alignment jitter.

For non-rectangular switching windows, Figure 8 shows no probability peak at low normalized powers, because no zero amplitude occurs in the pulse at the NOLM input in the absence of noise. Also, it can be observed that for low normalized powers, the PDF of the Gaussian-shaped pulse at the NOLM input has the lowest amplitude. This is a consequence of the lower steepness of the switching window amplitude resulting from the Gaussian-shaped pulse rather than the steepness of the switching window resulting from a super-Gaussian or rectangular-shaped pulse at the NOLM input. As a result, since the optimum decision threshold occurs for low normalized powers, the BER increases when the steepness of the pulse at the NOLM input increases. Figure 8b shows the PDFs of $a_{out,w}$ at the second regenerator output for different shapes of the pulse at the NOLM input. Compared with Figure 8a, it can be observed that the increase of the left-hand tail of the PDF of bit '1' is higher for the Gaussian-shaped pulse than for the other two shapes. This results from the higher amplitude fluctuations caused by the alignment jitter for the Gaussian-shaped pulse, which increase the PDF amplitude for moderate normalized powers, as can be seen in Figure 8a. As a result, the amplitude fluctuations combined with the noise added in the regeneration section lead to a higher increase of the left-hand tail in the PDF of bit '1'. This behavior is also responsible for the higher increase rate of the BER with m for the case of a switching window resulting from a Gaussian-shaped pulse.

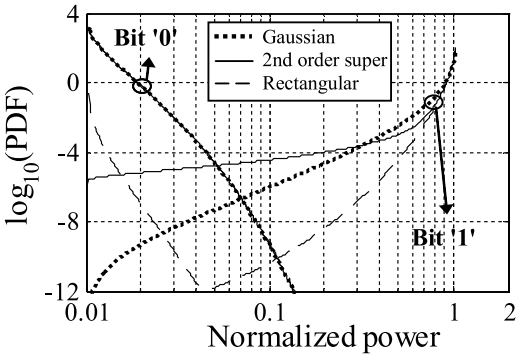

(a)

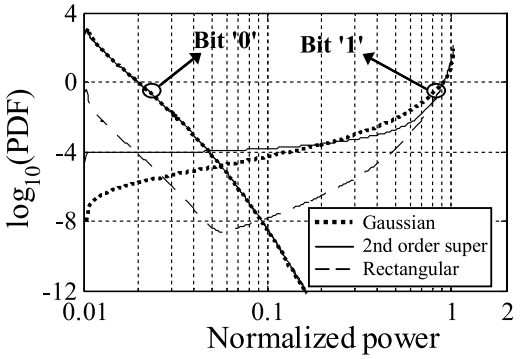

(b)

Figure 8. PDF of $a_{out,w}$ for different shapes of the signal at the NOLM input, $x_{th,NL} = 0.5$ (case 2), $D_{sw} = 0.75 \cdot T$ $(3.75 \cdot D_c)$, and $\sigma_j = 600$ fs: (a) $m = 1$ and (b) $m = 2$.

For lower alignment jitter variance and lower D_{sw} than in Figure 7, Figure 9 shows the BER at the output of the mth regenerator for different shapes of the pulse at the NOLM input, $\sigma_j = 300$ fs and $D_{sw} = 0.5 \cdot T$ $(2.5 \cdot D_c)$. As expected, the alignment jitter has a lower impact on the BER in Figure 9 than in the case of Figure 7. Thus, after a few regeneration sections, the noise accumulation dominates the BER degradation. Even when the noise accumulation dominates the BER degradation only for the switching window resulting from the Gaussian-shaped pulse, a small additional degradation is observed relative to the case in the absence of timing jitter. This degradation results from the higher amplitude fluctuations caused by the less-flattened switching window.

The BER along the chain of regenerators was also studied for $\sigma_j = 100$ fs and $D_{sw} = 0.5 \cdot T$ $(2.5 \cdot D_c)$ and for $\sigma_j = 300$ fs and $D_{sw} = 0.75 \cdot T$ $(3.75 \cdot D_c)$. For $\sigma_j = 100$ fs, the alignment jitter variance is too low, and the BER is only limited by the accumulated noise. In the case of $\sigma_j = 300$ fs, it was observed that as D_{sw} increases, the impact of the alignment jitter on the performance is lessened, and the performance is mainly limited by the accumulated noise.

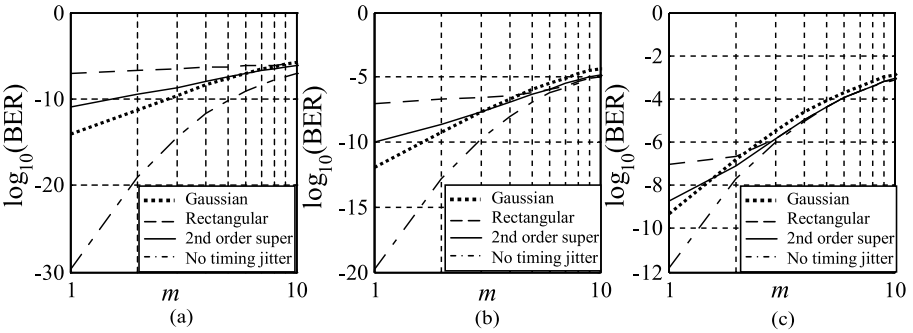

Figure 9. $\log_{10}(BER)$ as a function of m for the optimum $x_{th,NL}$, different shapes of the pulse at the NOLM input, $D_{sw} = 0.5 \cdot T$ $(2.5 \cdot D_c)$ and $\sigma_j = 300$ fs and 0 fs: (a) case 1. (b) case 2, and (c) case 3.

5. Conclusion

A numerical method to estimate the BER and the PDFs of the regenerator output signal at the sampling time instant along the chain of 3R all-optical regenerators based on non-linear gates has been proposed. Monte Carlo simulations have shown that for a few regenerators, or when the FWHM of the clock pulse is much lower than the switching window ($D_c \leq 0.2 \cdot D_{sw}$), the BER estimates provided by this method are quite accurate. However, in the case of very short clock pulses and at the first regenerator output, the proposed method provides BER estimates in excellent agreement with the BER estimates of Monte Carlo simulation. Therefore, the proposed method is a useful tool to understand the impact of the noise redistribution and amplitude fluctuations due to alignment jitter on the BER of a chain of 3R all-optical regenerators based on non-linear gates.

The impact of switching window shape on the BER of a chain of 3R all-optical regenerators based on the NOLM with a pulse reshaper has been numerically investigated with the proposed method. It has been shown that, contrary to what is usually stated in the literature, the rectangular switching window is not the most appropriate for a 3R regenerator. In fact, the optimum shape of the switching window depends on the number of regenerators of the chain, noise power, and alignment jitter level.

References

1. Simon, J.-C., Gay, M., Bramerie, L., Roncin, V., Joindot, M., Chartier, T., Lobo, S., Girault, G., Le, Q. T., Nguyen, T. N., and Ngo, M. N. 2008. Long distance transmission using optical regeneration. Paper no. OWS1. *Proceedings of the Optical Fiber Communication/National Fiber Optic Engineers Conference (OFC/NFOEC)*, San Diego, CA, February 24–28.
2. Leclerc, O., Lavigne, B., and Chiaroni, D. 2002. All optical regeneration: Principles and WDM implementation. *Optical Fiber Telecommunications IV-A Components*, San Diego, CA: Academic Press, chapter 15.
3. Ciaramella, E., and Giorgi, L. 2006. System performance using different types of in-line optical regenerators. *IEEE/OSA Journal of Lightwave Technology* 24(10):3727–3733.
4. Leiria, M. R. G., and Cartaxo, A. V. T. 2008. Impact of the signal and nonlinearity extinction ratios on the design of non-ideal 2R all-optical regenerators. *IEEE/OSA Journal of Lightwave Technology* 26(2):276–286.

5. Hainberger, R., Hoshida, T., Watanabe, S., and Onaka, H. 2004. BER estimation in optical fiber transmission systems employing all-optical 2R regenerators. *IEEE/OSA Journal of Lightwave Technology* 22(3):746–754.
6. Öhman, F., and Mørk, J. 2006. Modeling of bit error rate in cascaded 2R regenerators. *IEEE/OSA Journal of Lightwave Technology* 24(2):1057–1063.
7. Ohlén, P., and Berglind, E. 1997. Noise accumulation and BER estimates in concatenated nonlinear optoelectronic repeaters. *IEEE Photonics Technology Letters* 9(7):1011–1013.
8. Bischoff, S., Buxens, A., Fischer, S., Dülk, M., Clausen, A., Poulsen, H., and Mørk, J. 2001. Comparison of all-optical co- and counter-propagating high Mach-Zehnder interferometers. *Optical and Quantum Electronics* 33(7–10):907–926.
9. Shi, H., and Lin, J. 1999. Theoretical analysis on polarization deviation and switch window optimization in nonlinear optical loop mirror demultiplexer. *IEEE/OSA Journal of Lightwave Technology* 17(12):2572–2576.
10. Lee, J. H., Oxenløwe, L. K., Ibsen, M., Berg, K. S., Clausen, A. T., Richardson, D. J., and Jeppesen, P. 2003. All-optical TDM data demultiplexing at 80 Gb/s with significant timing jitter tolerance using a fiber bragg grating based rectangular pulse switching technology. *IEEE/OSA Journal of Lightwave Technology* 21(11):2518–2523.
11. Slavík, R., Oxenløwe, L. K., Galili, M., Mulvad, H. C. H., Park, Y., Azaña, J., and Jeppesen, P. 2007. Demultiplexing of 320-Gb/s OTDM data using ultrashort flat-top pulses. *IEEE Photonics Technology Letters* 19(22):1855–1857.
12. Uchiyama, K., Morioka, T., Kawanishi, S., Takara, H., and Saruwatari, M. 1997. Signal-to-noise ratio analysis of 100 Gb/s demultiplexing using nonlinear optical loop mirror. *IEEE/OSA Journal of Lightwave Technology* 15(2):194–201.
13. Weber, H.-G., Ludwig, R. Ferber, S., Schimidt-Langhorst, C., Kroh, M., Marembert, V., Boerner, C., and, Schubert, C. 2006. Ultrahigh-speed OTDM-transmission technology. *IEEE/OSA Journal of Lightwave Technology* 24(12):4616–4626.
14. Daikoku, M., Miyazaki, T., Morita, I., Hattori, T., Tanaka, H., Kubota, F., and Suzuki, M. 2009. 160 Gb/s-based field transmission experiments using polarizer-based PMD compensator with optical power monitor. *IEEE/OSA Journal of Lightwave Technology* 27(5):451–459.
15. Rochette, M., Kutz, J., Blows, J., Moss, D., Mok, J., and Eggleton, B. 2005. Bit-error-ratio improvement with 2R optical regenerators. *IEEE Photonics Technology Letters* 17(4):908–910.
16. Bigo, S., Leclerc, O., and Desurvire, E. 1997. All-optical fiber signal processing and regeneration for soliton communications. *IEEE Journal of Selected Topics in Quantum Electronics* 3(5):1208–1222.
17. Kang, K. I., Chang, T. G., Glesk, I., and Prucnal, P. R. 1996. Comparison of Sagnac and Mach-Zehnder ultrafast all-optical interferometric switches based on a semiconductor resonant optical nonlinearity. *Applied Optics* 35(3):417–426.
18. Gavioli, G., Thomsen, B., Mikhailov, V., and Bayvel, P. 2007. Cascadability properties of optical 3R regenerators based on SOAs. *IEEE/OSA Journal of Lightwave Technology* 25(9):2766–2775.
19. Carlson, A. B. 1986. *Communication Systems, An Introduction to Signal and Noise in Electrical Communication*. Singapore: McGraw-Hill, pp. 132–133.
20. Parmigiani, F., Petopoulos, P., Ibsen, M., and Richardson, D. J. 2006. All-optical pulse reshaping and retiming systems incorporating pulse shaping fiber Bragg grating. *IEEE/OSA Journal of Lightwave Technology* 24(1):357–364.
21. Lavigne, B., Renaudier, J., Lelarge, F., Legouezigou, O., Gariah, H., and Duan, G.-H. 2007. Polarization-insensitive low timing jitter and highly optical noise tolerant all-optical 40-GHz clock recovery using a bulk and a quantum-dots-based self-pulsating laser cascade. *IEEE/OSA Journal of Lightwave Technology* 25(1):170–176.
22. Jinno, M. 1994. All optical signal regularizing/regeneration using a nonlinear fiber Sagnac interferometer switch with signal-clock walk-off. *IEEE/OSA Journal of Lightwave Technology* 12(9):1648–1659.

23. Trischitta, P., and Varma, E. 1989. Jitter in digital transmission systems. Boston: Artech House.
24. Proakis, J. G. 1995. *Digital Communications*. Singapore: McGraw-Hill, pp. 41–45.
25. Sakamoto, T., and Kikuchi, K. 2004. Nonlinear optical loop mirror with an optical bias controller for achieving full-swing operation of gate switching. *IEEE Photonics Technology Letters* 16(2):545–547.

Biographies

Mário R. G. Leiria was born in Faro, Portugal, in 1978. He received his "licenciatura" degree in electrical and computer engineering in 2001 and his M.Sc. in electrical and computer engineering in 2003, both at the Instituto Superior Tecnico of Technical University of Lisbon. Currently, he is working toward his Ph.D. in electrical and computer engineering at the Instituto Superior Tecnico of Technical University of Lisbon. His research interests include performance assessment of transparent optical networks and 3R all-optical regeneration.

Adolfo Cartaxo was born in Montemor-o-Novo, Portugal, on January 10, 1962. He received his degree of "Licenciatura" in electrical and computer engineering, his M.Sc. degree in telecommunications and computers, and his Ph.D. in electrical and computer engineering in 1985, 1989, and 1992, respectively, from the Instituto Superior Técnico (IST), faculty of engineering of Lisbon Technical University. His Ph.D. work focused on clock recovery circuit optimization in the direct detection optical communications. In February 2005, he got his "Agregação" degree in electrical and computer engineering at IST. In 1985, he joined the Department of Electrical and Computer Engineering at IST. In 1992, he became an assistant professor and he was promoted to associate professor in January 2002. He joined the Optical Communications Group of Lisbon Pole of Instituto de Telecomunicações (IT) as a researcher in 1993. He is now a senior researcher conducting research on dense wavelength division multiplexed systems and networks. Since January 2002, he is a member of the National Coordination Commission on Optical Communications of IT. He has been a leader, technical auditor, and evaluator of multiple national and international programs in R&D in the optical communications area, including "Advanced Communications Technologies and Services: European RTD" (ACTS) and "Information Society Technologies" (IST). He has served as a reviewer for multiple international publications in the area of optical communications and networks, has authored or co-authored more than 50 journal publications (15 as first author), and published more than 80 international conference papers. He is the co-author of two international patents and is a senior member of the IEEE Laser and Electro-Optics Society. His main present research interests include fiber optic communication systems and networks.

Appendix A. Method of PDF Estimation along the Chain of Regenerators

The 3R regenerator output power is approximated by upper and under stair-case functions with amplitude given by the discrete set of levels $\{x_i\}$, with $1 \leq i \leq N$, as shown in Figure A1a. As a result of the stair-case approximation, $a_{out,w}$ conditioned on transmitted bit 'b' is described by the probability of assuming each level $\{x_i\}$ instead of its PDF. The error associated with this approximation is very small when the number of discrete values N is sufficiently high. Furthermore, Figure A1a shows that, in the upper stair-case approximation, the output power in the interval $[x_{i-1};\ x_i]$ is approximated by a constant

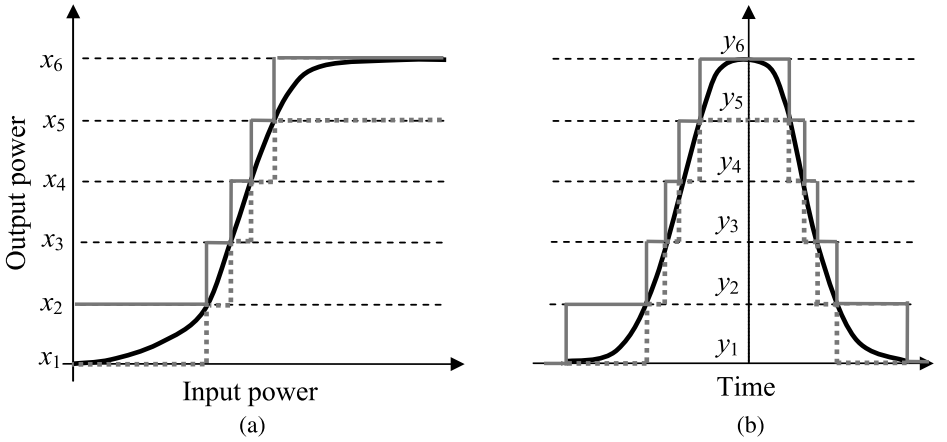

Figure A1. (a) Nonlinear characteristic of the regenerator and (b) example of a pulse prior to the nonlinearity, both in the solid black line. Upper stair-case approximation (solid gray line) and under stair-case approximation (dotted gray line) for $\{x_i\}$ and $\{y_k\}$ composed by six elements.

amplitude x_i, while, in the under-stair case approximation, it is approximated by x_{i-1}. Thus, using expression (13), the probability of $a_{out,w}$ conditioned on transmitted bit 'b' for each level $\{x_i\}$, using the upper stair-case approximation, is given by

$$\begin{aligned} p_{out,w,+}[i] &= \int_{x_{i-1}}^{x_i} f_{a_{out,w}}(z|\text{`}b\text{'})dz \\ &= \frac{a_{at}}{|d|^2}\sum_{c=1}^{C_p}\left[\int_{x_{i-1}}^{x_i}\left|\int_{z^{-1}_{n,s,w,c}(t_{c,-})}^{z^{-1}_{n,s,w,c}(t_{c,+})} f_{z_n}\left(F^{-1}_{NL}\left(\frac{a_{at}z}{|d|^2}\right)\right| z_{n,s,w}(t)=v_c\right)\right. \\ &\qquad \cdot \left|\frac{dF^{-1}_{NL}(y)}{dy}\right|_{y=\frac{a_{at}\cdot z}{|d|^2}} \cdot \left|\frac{dz^{-1}_{n,s,w,c}(y)}{dy}\right|_{y=v_c} \\ &\qquad \left. f_{jit}(z^{-1}_{n,s,w,c}(v_c))dv_c\right| dz\Bigg], \end{aligned} \tag{A1}$$

where the index + means that the upper stair-case approximation is considered. Expression (A1) can be simplified by making the substitution $\upsilon = F^{-1}_{NL}(a_{at}z/|d|^2)$. However, $F_{NL}(x)$ may be non-monotonic and must be split into monotonic functions [19]. Designating by C the number of subdivided monotonic functions, $F_{NL,h}(x)$ the hth subdivided monotonic function, and making the substitution $\upsilon = F^{-1}_{NL}(a_{at}z/|d|^2)$, gives

$$\begin{aligned} p_{out,w,+}[i] = \sum_{c=1}^{C_p}&\left|\int_{z^{-1}_{n,s,w,c}(t_{c,-})}^{z^{-1}_{n,s,w,c}(t_{c,+})} \frac{dz^{-1}_{n,s,w,c}(y)}{dy}\right|_{y=v_c} f_{jit}(z^{-1}_{n,s,w,c}(v_c)) \\ &\cdot \sum_{h=1}^{C}\left|\int_{F^{-1}_{NL,h}(a_{at}x_{i-1}/|d|^2)}^{F^{-1}_{NL,h}(a_{at}x_i/|d|^2)} f_{z_n}(\upsilon|z_{n,s,w}(t)=v_c)d\upsilon\right| dv_c\Bigg|. \end{aligned} \tag{A2}$$

The modulus was inserted in the term of the second sum of expression (A2), because each probability contribution cannot be negative. Otherwise, the integration limits have to be changed depending if the hth subdivided monotonic function is increasing or decreasing.

To take into account the effect of the alignment jitter, it is assumed that the signal power at the non-linearity input in the absence of noise is also approximated by upper and under stair-case functions with a discrete set of levels given by $\{y_k\}$, with $1 \leq k \leq M$, as shown in Figure A1b. Consequently, $z_n(t)$ conditioned on $z_{n,s,w}(t)$ is also described by a probability vector instead of its PDF. Thus, the integrations over v_c, with $1 \leq c \leq C_p$ in expression (A2), can be expressed as a sum. The probability of $a_{out,w}$ conditioned on the transmitted bit 'b' for each level $\{x_i\}$, considering an upper stair-case approximation for the regenerator output power and for $z_{n,s,w}(t)$, is approximated by

$$p_{out,w,+}[i] = \sum_{k=2}^{M} \left[\sum_{c=1}^{C_p} \left| \int_{v_{l,k,c}}^{v_{u,k,c}} \left. \frac{dz_{n,s,w,c}^{-1}(y)}{dy} \right|_{y=v_c} f_{jit}(z_{n,s,w,c}^{-1}(v_c)) \right. \right.$$
$$\left. \left. \sum_{h=1}^{C} \left| \int_{F_{NL,h}^{-1}(a_{at}x_{i-1}/|d|^2)}^{F_{NL,h}^{-1}(a_{at}x_i/|d|^2)} f_{z_n}(v|z_{n,s,w}(t) = y_k) dv \right| dv_c \right| \right], \quad \text{(A3)}$$

where

$$v_{u,k,c} = \begin{cases} z_{n,s,w,c}^{-1}(t_{c,+}) & y_k > z_{n,s,w,c}^{-1}(t_{c,+}) \\ y_k & y_k \leq z_{n,s,w,c}^{-1}(t_{c,+}) \end{cases} \quad \text{(A4)}$$

and

$$v_{l,k,c} = \begin{cases} z_{n,s,w,c}^{-1}(t_{c,-}) & y_{k-1} < z_{n,s,w,c}^{-1}(t_{c,-}) \\ y_{k-1} & y_{k-1} \geq z_{n,s,w,c}^{-1}(t_{c,-}) \end{cases}. \quad \text{(A5)}$$

The two options for $v_{u,k,c}$ and $v_{l,k,c}$ result from the fact that the interval between y_{k-1} and y_k may contain several monotonic parts of $z_{n,s,w}(t)$. Due to the upper stair-case approximation for $z_{n,s,w}(t)$, the sum over k starts at $k = 2$.

Expression (A3) describes the probability of the output power at the sampling time instant for each level $\{x_i\}$, due to the effects of noise and alignment jitter. In a chain of regenerators, the peak power of the pulses at the regenerator input $|b_w|^2$ is the same as the peak power of the pulses at the regenerator output $a_{out,w}$ of the previous regenerator, as discussed in Section 3.1. Thus, the probability vector of $|b_w|^2$ conditioned on the transmitted bit 'b', $p_{in,w}[j]$, is equal to the probability of $a_{out,w}$ conditioned on the transmitted bit 'b' for each level $\{x_i\}$ of the previous regenerator with $i = j$.

From expression (9), it can be seen that $z_{n,s,w}(t)$ depends on $|b_w|^2$. Thus, the integration limits of the PDF of the alignment jitter in expression (A3) depend on $|b_w|^2$. Taking into consideration that the amplitude of $|b_w|^2$ is also described by a probability vector $p_{in,w,+}[j]$ (in the upper stair-case approximation), the probability of $a_{out,w}$ conditioned on the transmitted bit 'b' for each level $\{x_i\}$ is obtained by statistically averaging expression (A3) over $p_{in,w,+}[j]$. Thus, for the upper stair-case approximation and making the substitution $z_c = z_{n,s,w,c}^{-1}(v_c)$ for $1 \leq c \leq C_p$ in the corresponding integral

of expression (A3), the probability of $a_{out,w}$ conditioned on the transmitted bit 'b' for each level $\{x_i\}$ is given by

$$p_{out,w,+}[i] = \sum_{j=1}^{N} \left(\sum_{k=2}^{M} \left[\sum_{c=1}^{C_p} \left| \int_{z^{-1}_{n,s,w,c}(v_{l,k,c})||b_w|^2=x_j}^{z^{-1}_{n,s,w,c}(v_{u,k,c})||b_w|^2=x_j} f_{jit}(z_c)dz_c \right| \right. \right.$$
$$\left. \left. \cdot \sum_{h=1}^{C} \left| \int_{F^{-1}_{NL,h}(a_{at}x_{i-1}/|d|^2)}^{F^{-1}_{NL,h}(a_{at}x_i/|d|^2)} f_{z_n}(v|z_{n,s,w}(t) = y_k)dv \right| \right] \cdot p_{in,w,+}[j] \right), \tag{A6}$$

where $z^{-1}_{n,s,w,c}(v)||b_w|^2 = x_j$ is the value of $z^{-1}_{n,s,w,c}(v)$ when $|b_w|^2 = x_j$. Let l_{ik} be the probability, due to the noise, that $a_{out,w}$ is equal to x_i conditioned by the fact that $z_{n,s,w}(t)$ is y_k. Then, l_{ik} is given by

$$l_{ik} = \begin{cases} \sum_{h=1}^{C} \left| \int_{F^{-1}_{NL,h}(a_{at}x_{i-1}/|d|^2)}^{F^{-1}_{NL,h}(a_{at}x_i/|d|^2)} f_{z_n}(v|z_{n,s,w}(t) = y_k)dv \right| & i > 1 \\ 0 & i = 1 \end{cases}. \tag{A7}$$

Furthermore, let h_{kj} be the probability, due to alignment jitter, that $z_{n,s,w}(t)$ is equal to y_k conditioned by the fact that $|b_w|^2$ is x_j. Then, h_{kj} is given by

$$h_{kj} = \begin{cases} \sum_{c=1}^{C_p} \left| \int_{z^{-1}_{n,s,w,c}(v_{l,k,c})||b_w|^2=x_j}^{z^{-1}_{n,s,w,c}(v_{u,k,c})||b_w|^2=x_j} f_{jit}(z_c)dz_c \right| & k > 1 \\ 0 & k = 1 \end{cases}. \tag{A8}$$

Replacing expressions (A7) and (A8) in expression (A6) gives

$$p_{out,w,+}[i] = \sum_{j=1}^{N} \left[\sum_{k=2}^{M} (l_{ik} \cdot h_{kj}) \cdot p_{in,w,+}[j] \right]. \tag{A9}$$

Using matrix notation, expression (A9) can be written as

$$p_{out,w,+}[i] = (L[l_{ik}] \otimes H[h_{kj}]) \otimes p_{in,w,+}[j], \tag{A10}$$

where $L[l_{ik}]$ and $H[h_{kj}]$ are the probability transfer matrices, and $\otimes$ is the matrix multiplication operation.

In the case of the under stair-case approximation, following the same steps as for expression (A6), the probability of $a_{out,w}$ conditioned on the transmitted bit 'b' for each level $\{x_i\}$ is given by

$$p_{out,w,-}[i] = \sum_{j=1}^{N} \left[\sum_{k=2}^{M} (l_{(i+1)(k-1)} \cdot h_{kj}) \cdot p_{in,w,-}[j] \right], \tag{A11}$$

where $p_{in,w,-}[j]$ is the probability vector of the signal at the regenerator input for the under stair-case approximation. As for expression (A9), expression (A11) can be also written in matrix notation.

Recalling that the stair-case function with amplitude x_i corresponds to the interval $[x_{i-1}; x_i]$ in the upper stair-case approximation and to the interval $[x_i; x_{i+1}]$ in the under stair-case approximation, the probability vector of $a_{out,w}$ conditioned on the transmitted bit 'b' is converted to the discrete PDF of $a_{out,w}$ conditioned on the transmitted bit 'b' by

$$f_{out,w,+}[i] = p_{out,w,+}[i]/(x_i - x_{i-1}) \tag{A12}$$

and

$$f_{out,w,-}[i] = p_{out,w,-}[i]/(x_{i+1} - x_i). \tag{A13}$$